



HAL
open science

Comparison of pXRF and LA-ICP-MS analysis of lead-rich glass mosaic tesserae

Laura Ware Adlington, Bernard Gratuze, Nadine Schibille

► **To cite this version:**

Laura Ware Adlington, Bernard Gratuze, Nadine Schibille. Comparison of pXRF and LA-ICP-MS analysis of lead-rich glass mosaic tesserae. *Journal of Archaeological Science: Reports*, 2020, 34, Part A, pp.102603. 10.1016/j.jasrep.2020.102603 . hal-02967327

HAL Id: hal-02967327

<https://hal.science/hal-02967327>

Submitted on 2 Jul 2021

HAL is a multi-disciplinary open access archive for the deposit and dissemination of scientific research documents, whether they are published or not. The documents may come from teaching and research institutions in France or abroad, or from public or private research centers.

L'archive ouverte pluridisciplinaire **HAL**, est destinée au dépôt et à la diffusion de documents scientifiques de niveau recherche, publiés ou non, émanant des établissements d'enseignement et de recherche français ou étrangers, des laboratoires publics ou privés.



Comparison of pXRF and LA-ICP-MS analysis of lead-rich glass mosaic tesserae

L.W. Adlington^{a,*}, B. Gratuze^a, N. Schibille^{a,*}

^a IRAMAT-CEB, UMR5060, CNRS, 3D rue de la Férollerie, 45071 Orléans, cedex 2, France

ARTICLE INFO

Keywords:

High lead glass
handheld XRF
Surface analysis
LA-ICP-MS
Archaeology

ABSTRACT

Handheld (portable) X-ray fluorescence spectrometry (pXRF) allows for fast, in situ surface analysis, however, its application in archaeological research requires substantial optimisation. This paper investigates the matrix effects of high lead glass on the experimental results of pXRF in comparison to laser ablation inductively coupled plasma mass spectrometry (LA-ICP-MS) data. 289 archaeological glass mosaic tesserae with varying lead concentrations up to 35 wt% PbO were systematically analysed by both techniques. In addition, thirteen reference glasses were analysed, including nine glass standards (BGIRA1-6 and AD1-3), which were not previously reported.

The detection of low Z elements (Ca and above) was inaccurate in both low- and high-lead tesserae, due to a shallow depth of analysis and suboptimal surface conditions of archaeological glass. The presence of relatively low concentrations of lead (<0.5 wt%, depending on the element being measured) furthermore resulted in overlapping peaks. The limits of detection as well as accuracy for several trace elements were severely affected by high lead contents, leading to over- or underestimations.

Separate empirical calibrations for low- and high-lead glasses were effective in correcting the data, and this approach is recommended for any study using pXRF to analyse glass assemblages, especially those containing variable concentrations of lead. We also advise that in addition to the analysis of reference materials a subset of an assemblage is analysed by another analytical technique, to assess the performance of the spectrometer and to establish a robust calibration protocol. Overall our results suggest that pXRF can be used as a survey technique to differentiate compositional groups and inform further sampling. Even though the identification of specific glass groups requires major element compositions, different primary glass types and colouring/opacifying techniques can be discriminated.

1. Introduction

The development of a handheld (portable) X-ray fluorescence spectrometer (pXRF) has opened up new analytical options for scientists, curators and conservators working within the archaeology and cultural heritage sectors. The primary benefits are its capability for in situ analysis, its short acquisition time, and the relatively low cost of the machine. It can be transported to an object in a museum or on excavation, bypassing restrictions on invasive sampling or exportation of objects or samples. The speed of analysis allows the examination of hundreds of samples in a relatively short period of time, making it an appealing tool for conducting a survey of a large assemblage. As a result of these advantages, the technique is used around the world on a range of archaeological materials (Adlington and Freestone, 2017;

Dungworth, 2012; Gabler, 2017; Grave et al., 2012; Heginbotham et al., 2019; Heginbotham and Solé, 2017; Janssens et al., 2016; Koleini et al., 2020, 2017; Martínón-Torres et al., 2012; O'Grady and Hurst, 2011; Roxburgh et al., 2018; Tykot, 2016).

The portability of pXRF comes at the cost of data quality, due in large part to the lack of sample preparation and lack of a vacuum during analysis, requiring a critical assessment of its performance. Studies comparing handheld spectrometers and laboratory-based XRF systems have shown that handheld systems generally compare favourably in terms of precision for certain materials such as obsidian (Craig et al., 2007; Goodale et al., 2012), although weathering on the surface of an artefact can adversely affect the results (Adlington and Freestone, 2017; Williams-Thorpe et al., 1999). Furthermore, the accuracy of the absolute concentrations generated by a spectrometer's

* Corresponding authors.

E-mail addresses: laura.adlington.12@ucl.ac.uk (L.W. Adlington), nadine.schibille@cnrs-orleans.fr (N. Schibille).

<https://doi.org/10.1016/j.jasrep.2020.102603>

Received 16 July 2020; Received in revised form 23 September 2020; Accepted 25 September 2020

2352-409X/© 2020 The Author(s). Published by Elsevier Ltd. This is an open access article under the CC BY-NC-ND license

(<http://creativecommons.org/licenses/by-nc-nd/4.0/>).

built-in calibrations can be problematic (Brand and Brand, 2014; Sheppard et al., 2011), although the accuracy of the data can be corrected with additional linear calibration if the precision is sufficient. The successful application of pXRF depends upon a thorough understanding of how the spectrometer works and the sample material; yet the ease of use means anyone can easily generate a table of data about their material (Scott et al., 2012). The potential for misuse has resulted in scepticism towards the technique and its application in archaeology (Brand and Brand, 2014; Frahm, 2013; Goodale et al., 2012; Liritzis and Zacharias, 2011; Shackley, 2010; Speakman and Shackley, 2013; Stroth et al., 2019).

The analysis of glass by pXRF is made difficult by the lack of a vacuum, preventing the detection of light elements, such as Na, Mg, Al and Si, which make up the bulk of most glass. Some systems may be used with a helium flush that allow the measurement of elements as light as Na (Kaiser and Shugar, 2012). However these data are most likely to be heavily influenced by the surface conditions of the object. Deterioration or accumulated corrosion products create layers of material that do not match the bulk composition. These layers disproportionately affect the measurement of low Z elements or elements read from low energy characteristic X-rays (Kaiser and Shugar, 2012). In other words, light elements, which make up the bulk of most glass, are more heavily influenced by deterioration or surface decorations, and possibly cannot be quantified as a characterisation of the bulk composition. This problem has been addressed in the study of medieval and post-medieval glass by focusing on the measurement of heavy trace elements Rb, Sr and Zr (Adlington and Freestone, 2017; Dungworth, 2012), which have been used to distinguish broad compositional and technological glass types as well as recipe deviations. Furthermore, small sample size, thin samples and irregular surfaces may affect analysis by pXRF. The impact of minor irregularities, such as rough, bumpy or curved surfaces, may be corrected by normalising the intensity of the characteristic X-rays to scatter peaks (Potts et al., 1997; Wilke et al., 2016). A study exploring the usefulness of pXRF for obsidian sourcing using suboptimal conditions, including reliance on the machine's built-in quantifications and samples that were small and irregularly shaped, yielded overall satisfactory results (Frahm, 2013).

Another significant obstacle to the use of pXRF is the matrix effects associated with glasses containing moderate or high amounts of lead. Even relatively minor concentrations of lead in a glass can interfere with the measurement of arsenic, for example, which is often quantified using the $K\alpha$ line (10.54 keV; Bearden, 1967) that is overlapped by the lead $L\alpha$ line (10.55 keV). At higher concentrations, there is a greater likelihood that elemental concentrations measured from X-rays close to lead emission lines will be affected. Furthermore, the greater density of a high lead glass affects the Rayleigh and Compton scatter peaks as well as the depth of analysis for all elements (Kaiser and Shugar, 2012).

This study systematically investigates the effects of lead contents on pXRF analyses of an assemblage of early Islamic mosaic tesserae by comparing the pXRF results with data obtained by laser ablation inductively coupled plasma mass spectrometry (LA-ICP-MS). Several matrix-matched reference materials were also analysed to discriminate effects attributable to the surface conditions of the tesserae, and those attributable to matrix effects associated with lead. Using this approach, we seek to identify elements that might be commonly problematic in pXRF analyses of similar assemblages as well as those that have the greatest potential to be accurately measured. Recommendations for an appropriate methodological approach will be made and the potential usefulness of employing pXRF to study an assemblage containing lead-rich glass such as mosaic tesserae will be discussed (Arletti et al., 2011; Boschetti et al., 2016; Silvestri et al., 2014; Wypyski, 2005). Studies of mosaic tesserae stand to benefit enormously from pXRF analysis as it could be used to rapidly analyse hundreds of tesserae, even while in situ, and to identify groups of tesserae that may relate to different glass sources, recycling and/or later restoration campaigns,

and the data may be used for further sampling decisions. Finally, data for several glass standards not previously published are also made available.

2. Materials and methods

Our approach depends upon the characterisation of archaeological glass in addition to matrix-matched reference materials. It is difficult to acquire a sufficient number of suitable glass standards, which together contain all the elements in the full range of concentrations found in an archaeological assemblage. This difficulty is exacerbated for high lead glasses, for which the selection is even more limited. The characterisation of archaeological materials allows a greater number of data for a more robust investigation. Furthermore, while reference materials may be used to measure the performance of the pXRF spectrometer with an "ideal" sample – that is, a material that is flat, level, homogeneous, and in pristine condition – they cannot shed light on the performance of the spectrometer in the analysis of archaeological materials, which frequently do not meet these criteria. Therefore the characterisation of archaeological glass in this paper will provide a practical insight into the performance of pXRF under real conditions.

Since the archaeological tesserae studied in this paper were generally large enough to accommodate the pXRF spot size of 1 cm (diameter) as well as being sufficiently thick, and also had at least one surface that was suitably flat and level, most of the discrepancies between the pXRF and LA-ICP-MS data are expected to originate in poor surface conditions or high lead matrix effects. Another possible source of error is sampling uncertainty due to the heterogeneity of some tesserae, which can derive from the presence of large inclusions or phases. Many of the high lead tesserae are highly heterogeneous (e.g., Fig. 1) as a consequence of the production of certain colours. For example, to create yellow from lead antimonate, the pigment must be added at relatively low temperatures to avoid dissolution of the lead antimonate crystals, resulting in incomplete mixing (Lahlil et al., 2011, 2008; Shortland, 2002). Similarly, high temperatures can cause the dissolution of crystalline particles of lead-tin oxide and eventually the formation of SnO_2 crystals, converting the yellow colour into white (Matin et al., 2018). The resultant heterogeneity from incomplete mixing can present a problem for comparing analyses by pXRF and LA-ICP-MS. The analyses by pXRF (with its spot size of 1 cm in diameter) will encompass approximately the entire surface of the tessera, while analyses by LA-ICP-MS, with a beam width of 100 μm or less, take place over a much smaller area and can more easily avoid large inclusions and target individual phases in the glass. This may lead to poor agreement between the two techniques.

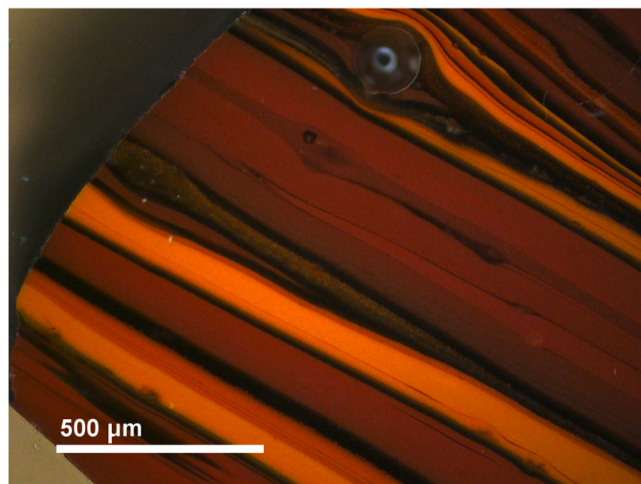


Fig. 1. Optical microscope image of a red tessera from the Roman villa in Noheda (Noheda 62; Schibille et al., 2020a) showing a heterogeneous microstructure.

2.1. Archaeological materials

The majority ($n = 270$) of the tesserae selected for this study are from Khirbat al-Minya, an early 8th-century Umayyad residence near Lake Tiberias (Israel) (Adlington et al., 2020; Ritter, 2017). LA-ICP-MS data identified these tesserae as having been made using natron as the primary flux, with some tesserae containing up to about 35 wt% PbO (Adlington et al., 2020). Some samples ($n = 19$) from the Roman villa in Noheda, Spain, were also included in order to better understand the impact of the presence of lead on the measurement of antimony. The LA-ICP-MS data of these samples have been published (Schibille et al., 2020a), and the selected tesserae include both natron-type glasses and plant ash glasses with moderate to high lead contents (about 5 wt%–35 wt% PbO).

2.2. Glass reference materials

Thirteen glass reference materials were used in this study to help confirm whether analysis of different elements were affected by surface conditions or matrix effects. The four Corning standards (Corning A-D) are widely used and can be compared to published values (Adlington, 2017; Brill, 1999; Wagner et al., 2012); of these, Corning C contains high lead (36.7 wt% PbO) as well as high barium (11.4 wt% BaO). Also included were six reference glasses from the British Glass Industry Research Association, BGIRA 1–6, which include three low-lead glasses (<0.01 wt% PbO) and three moderate- to high-lead glasses (3.5 wt%–33.1 wt% PbO). Neither the standards themselves nor their certified compositions are presently available from the manufacturer (now Glass Technology Services in Sheffield), however several laboratories appear to own samples of some or all of these glasses as they are referenced in published works, often without specifying which of the standards were used and almost always without reported compositions (Licenziati and Calligaro, 2016; Mao, 2000; Meek, 2016; Neri et al., 2018; Robinet et al., 2008; Tesser et al., 2020; Verità et al., 2018; Zucchiatti et al., 2002). Exceptions of which we are aware are published analyses of BGIRA 3 (de Viguierie et al., 2009) and BGIRA 4 (Bugoi et al., 2016). As data for these are not easily available, the pXRF measurements were thus compared to our own LA-ICP-MS data (Table S1). Electron microprobe data (EPMA-WDS) are also included in Table S1. Finally, three glass reference materials (AD1-3), designed to approximate medieval forest glass compositions (with high K_2O and CaO), were included in this study for their range of trace elements, although all contain <0.1 wt% PbO. The standards were prepared at the UCL Institute of Archaeology, melted by the Roman Glassmakers, and characterised by EPMA-WDS and LA-ICP-MS (Adlington, 2019). The current preferred compositions are given in Table S2 (Adlington, 2019) but may be subject to further minor modifications as the standards are part of an ongoing round-robin organised by L. Dussubieux (a follow up to the one published in Dussubieux, 2016). The standards are held at the Institute of Archaeology, UCL.

2.3. (Handheld) portable X-ray fluorescence spectrometry (pXRF)

Analyses were carried out using an Innov-X Systems/Olympus Delta Premium DP-6000CC handheld portable X-ray fluorescence spectrometer (pXRF), which has a Rh anode, a silicon drift detector, and a spot size of 1 cm. The tesserae were analysed on the surface after cleaning, using a test stand. The analyses were carried out using the proprietary “Soils” mode, which is optimised for oxygen-rich matrices using Compton normalisation for quantification of 30 elements from phosphorus through bismuth. The “Soils” mode uses three so-called “beams”, or settings with different combinations of primary radiation voltage, current and filters to target different regions of the spectrum. Beam 1 operates with a 40 kV accelerating voltage, 89 μA tube current, and a 1.5 mm copper filter; Beam 2 uses a 40 kV accelerating voltage, 52 μA tube current, and a 2.0 mm aluminium filter; and Beam 3 runs with a 15 kV accelerating voltage, 68 μA tube current, and a 0.1 mm aluminium filter.

Each beam was operated sequentially for 20 s for a total of 60 s analytical time per sample. In order to assess the quality of the data “straight from” the pXRF (Frahm, 2013), we rely solely on the built-in calibration programme with no further empirical calibrations applied to the data. The pXRF data are reported in Table S3.

2.4. Laser ablation inductively coupled mass spectrometry (LA-ICP-MS)

The Noheda tesserae and a subset of the Khirbat al-Minya tesserae were sampled by removing a small amount of material that was embedded in epoxy resin with the cross-section exposed and polished to remove any residue on the surface. The rest of the tesserae from Khirbat al-Minya were analysed after cleaning but without further sample preparation.

Analyses were carried out at IRAMAT-CEB using a Resonetics M50E excimer laser (ArF, 193 nm) with a S155 ablation cell and a Thermo Fisher Scientific ELEMENT XR mass spectrometer. The samples were ablated in spot-mode with a 5 mJ energy, a 10 Hz pulse frequency and a beam diameter typically set to 100 μm , occasionally reduced to 50 μm when saturation of the signal caused by high concentrations of manganese, copper, lead and/or tin or antimony particles occurred. Samples were pre-ablated for 20 s to remove any surface alterations, and the acquisition time was set at 30 s. The ablated material was transported to the plasma torch by an argon/helium flow at a rate of approximately 1 L/min for Ar and 0.65 L/min for He. A combination of internal (^{28}Si) and external standards (NIST SRM610, Corning glasses B, C, and D and an in-house APL1) were used for calibration and quantification, following the procedures described by Gratuze (1999). Instrumental precision and accuracy were monitored throughout the analyses by measuring reference materials (NIST SRM612, Corning A, B, C and D; Adlington, 2017; Jochum et al., 2011) at regular intervals (Adlington et al., 2020; Schibille et al., 2020a).

3. Results

The analyses by handheld pXRF were compared to accepted values (for the Corning and AD reference materials) and LA-ICP-MS data (for the BGIRA reference materials and the tesserae) in scatterplots showing a linear regression equation and the coefficient of determination (R^2 ; Figs. 2–7). The slope of the linear regression can be regarded as a proxy for accuracy; the closer this number is to 1, the more accurate the measurements are in general. Similarly, R^2 can be used as a proxy for precision. When R^2 is close to 1, the agreement is linear and reproducible. The pXRF analyses were also compared to the lead contents of each sample in order to determine whether lead contents affected the pXRF measurements due to overlapping peaks.

Several elements were well measured in terms of precision (R^2) in both the reference materials and the tesserae, regardless of lead content. Ti, Mn, Cu, Zn, Sb and Pb all had an R^2 better than 0.95 for the reference glasses; in the analyses of the tesserae, the R^2 were generally lower but all had an R^2 better than 0.9 except for Ti, with $R^2 = 0.84$ (Fig. 2). The pXRF overestimated concentrations of Ti in nine tesserae and one reference glass (AD2) (Fig. 2A–B), which introduces greater error into the measurement of this element. The source of this error is not clear, but is possibly due to the heterogeneity of some tesserae. Most of these nine tesserae are red, orange or yellow, which are highly heterogeneous and may have large phases and/or inclusions (Fig. 1). Coloured glasses have been found to have much more variable titanium concentrations than colourless counterparts (Schibille et al., 2018). Whatever the cause, without these nine outliers the precision in Fig. 2B is substantially improved ($R^2 = 0.94$). At least two tesserae were measured with elevated Mn contents, both of which were coloured with manganese (Fig. 2D). This again may reflect a high degree of heterogeneity of the colourants within the glass matrix. While the precision for these elements was good, the accuracy was much more variable, with slopes ranging from 0.73 to 1.26 (Fig. 2).

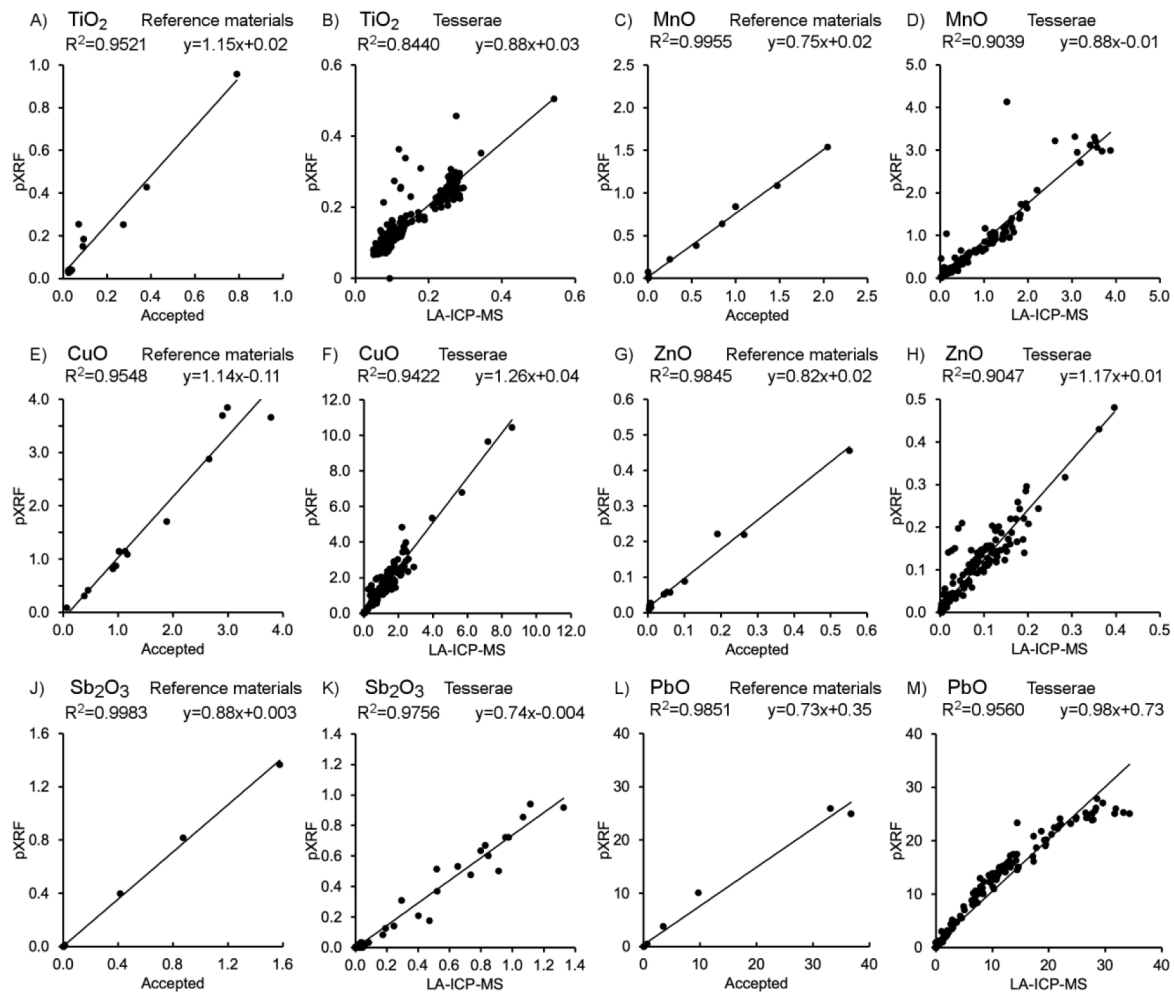


Fig. 2. Comparison of pXRF data with accepted values of reference glasses and with LA-ICP-MS data of archaeological tesserae for elements that were well measured in both the reference glasses and the tesserae. There are some outliers, most notably the several tesserae measured with higher TiO_2 (2B). Concentrations are all in oxide wt% for this figure.

3.1. Surface conditions and shallow depth of analysis

Phosphorus, potassium and calcium were well measured in the reference materials in terms of precision. In terms of accuracy, phosphorus and, to a lesser extent, potassium are systematically overestimated in the analyses of the reference materials. In the tesserae, both precision and accuracy of these three elements were poor, regardless of lead content (Fig. 3). While generally the upper range of the concentrations in the reference materials exceeds those found in the tesserae, especially for potassium, much of this error is attributed to the very shallow depth of analysis for these elements (Table 1), and the likely alteration of the surface composition due to the burial environment and deterioration.

3.2. Mismeasurement due to peak overlap

For several elements there was no correlation between the pXRF measurements and the LA-ICP-MS results (e.g., Fig. 4A); these elements were instead correlated with the Pb contents of the glass (Fig. 4B–D). The affected elements included S (based on analysis of reference materials only, as S was not analysed by LA-ICP-MS) and As, which are both commonly measured from peaks that overlap lead peaks (S-K α 2.31 keV with Pb-M α 2.35 keV, and As-K α 10.54 keV with Pb-L α 10.55 keV). Cd (K α 23.17 keV) also shows a positive correlation with Pb

contents, due to an overlap with the sum peak of the Pb-L α and Pb-L β lines (23.165 keV). Elements present in relatively low concentrations and that are measured from the low-energy region of the spectrum (e.g., Cl-K α 2.62 keV, La-L α 4.65 keV, and Ce-L α 4.84 keV) also show a positive correlation with lead contents; Cl overlaps with Pb-M γ (2.65 keV), while La and Ce appear to be affected by the presence of sum peaks of Pb-M lines. Measurements of Y show a positive correlation with lead contents in tesserae containing up to about 2 wt% PbO. Above this threshold the pXRF was below detection for Y (Fig. 4D; Y-K α 14.96 keV, Pb-L γ at 14.76 keV). It is important to stress that measurement of these elements is affected even at relatively low concentrations of lead. For example, La contents were highly overestimated by pXRF in glasses containing more than 2 wt% PbO. Even below this threshold the La readings were unreliable as some glass with PbO < 0.5 wt% were reported to have more than 100 ppm La.

The high barium contents (11.4 wt% BaO) of Corning C have a similar effect on the measurement of Ti (Ti-K α 4.51 keV; Ba-L α 4.47 keV), V (V-K α 4.95 keV; Ba-L β 4.83 keV) and Cr (Cr-K α 5.41 keV; Ba-L γ 5.53 keV; Fig. 5). Interference from Ba did not appear to adversely affect the analysis of the remainder of the reference glasses (BaO < 0.5 wt%) or any of the tesserae (BaO < 0.1 wt%); however, these peak interferences will be relevant to the study of ancient Chinese glasses (Henderson et al., 2018) and Late Islamic Arabian glazes (Zivković et al., 2019) with lead-barium composition.

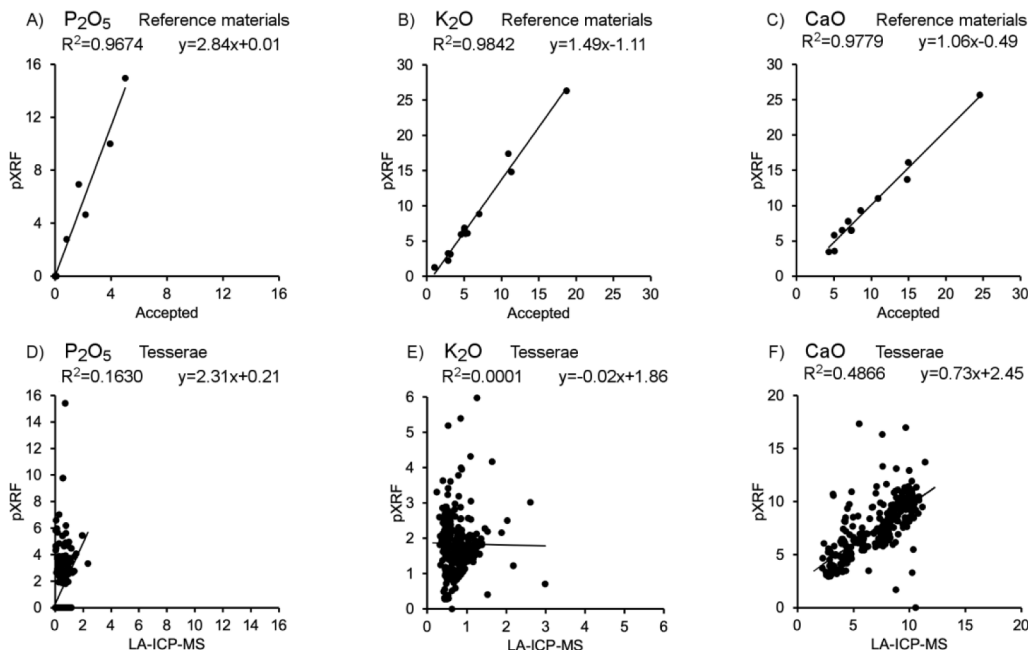


Fig. 3. Comparison of pXRF data with accepted values of reference glasses and with LA-ICP-MS data of archaeological tesserae for P, K, and Ca. These elements were well measured in the reference glasses in terms of precision, but poorly measured in the tesserae suggesting that poor surface conditions and shallow depths of analysis (Table 1) have affected the analyses by pXRF. Concentrations are all in oxide wt% for this figure.

Table 1

The critical depth of analysis, or the depth from which 99% of the characteristic X-rays are emitted, of selected elements in a low- and high-PbO tessera. Model calculations are based upon the chemical compositions of samples from Khirbat al-Minya (MR-T106 with < 0.01 wt% PbO and MR-T127 with 32 wt% PbO) and the spectrometer settings used in this study.

	Char. X-ray (keV)	Critical depth of analysis (µm) in	
		Low PbO tessera	High PbO tessera
P	2.01	11	8
K	3.31	38	14
Ca	3.69	52	18
Ti	4.51	83	27
Mn	5.90	174	52
Fe	6.40	219	64
Cu	8.05	371	113
Sr	14.17	1764	234
Zr	15.78	2351	234

3.3. Limits of detection and quantification (LOD/LOQ)

The limits of detection (LOD) and/or limits of quantification (LOQ) of some elements were raised in the presence of lead. Measurements of Co, Ni, Rb and Zr were below detection in reference materials and tesserae with elevated Pb concentrations, although the threshold varied. Co was below detection limits by pXRF in glasses containing more than about 3.5 wt% PbO; for Ni, this threshold was 1.5 wt% PbO; for Rb, 4.8 wt% PbO; and for Zr, glasses containing more than 2.5 wt% PbO were either significantly undermeasured or below detection.

Some of these elements were poorly quantified even in the low-lead glasses, suggesting a higher LOD or LOQ might be advisable for both high and low lead glasses. For example, Co was well measured in both reference materials and the tesserae when concentrations exceeded 100–200 ppm Co (Fig. 6A); these glasses generally contained <1–1.5 wt % PbO (no cobalt glasses with high lead concentrations could be found). Measurements of Co present at less than about 100 ppm were very poor (Fig. 6B). Similarly, Rb was well measured in the reference materials, which have concentrations up to almost 800 ppm Rb (Fig. 6C). The tesserae, however, contain Rb < 20 ppm, which adversely affected the

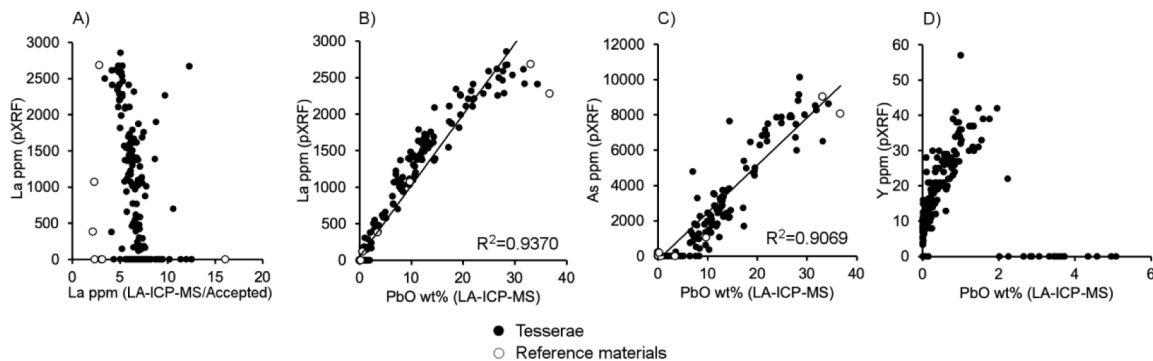


Fig. 4. Graphs demonstrating the effect of Pb peaks overlapping with other elements. (A) La concentrations measured by pXRF are not consistent with LA-ICP-MS data for La, but instead are correlated with Pb contents of the glass (B). As concentrations measured by pXRF are similarly correlated with Pb contents (C), while Y contents are correlated up to about 2 wt% PbO, and higher than this Y contents were reported as below detection. Legend below graphs.

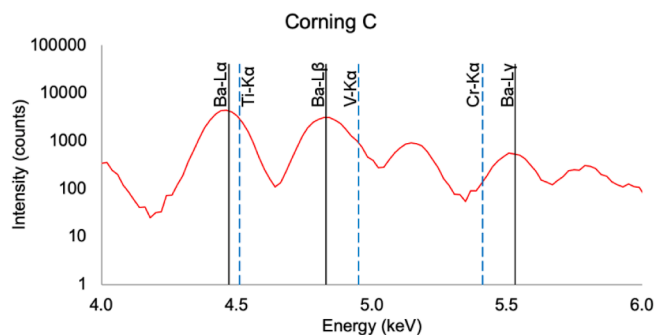


Fig. 5. Corning C spectrum between 4 and 6 keV, showing Ba peaks overlapping the K α lines of Ti, V and Cr.

precision ($R^2 = 0.43$) as the low concentrations approach the detection limits (Fig. 6D). Low concentrations of Ni also showed low precision (for Ni < 100 ppm, $R^2 = 0.57$; Fig. 6G–H).

Analysis of Zr in low lead glass by pXRF was excellent in terms of precision ($R^2 = 0.96$ for tesserae containing <2.5 wt% PbO) but very poor in accuracy ($m = 1.40$), underlining the need for empirical calibration on top of the machine quantification algorithm.

3.4. Elements requiring separate calibrations for different Pb concentrations

The measurement of some elements, most conspicuously Fe and Sr, would benefit from different calibrations for low- and high-lead glasses. For Fe, a different slope is observed for tesserae containing more than about 4.5 wt% PbO (Fig. 7A). Sr is undermeasured in glass with PbO greater than 7 wt% compared to glass with lower concentrations of PbO. A good linear agreement exists between the pXRF and LA-ICP-MS data for Sr for glass containing <7 wt% ($R^2 = 0.95$), and for glass 7 wt% to 14.3 wt% PbO ($R^2 = 0.93$; Fig. 7B). The linear relationship between the

pXRF and LA-ICP-MS data for Sr is weak for glass containing more than about 14.3 wt% ($R^2 = 0.67$), but these data might still be improved with empirical calibration (Fig. 7B).

4. Discussion

4.1. Methodological recommendations

Overall, the results are very promising as the use of pXRF for the study of lead-rich glass is only marginally more problematic than the study of low-lead glasses. The pXRF results of several elements were excellent in terms of precision. Elements impeded by peak overlap are typically affected even at low amounts of lead. The main obstacle to analysing high lead glasses is the increased LOD or LOQ of some elements. The inability to measure Zr or Rb in the presence of high lead concentrations is likely to be a limitation for many studies using pXRF on lead-rich glass.

Some elements were systematically over- or undermeasured in the presence of higher lead concentrations. The application of empirical calibrations is therefore particularly pertinent to assemblages containing variable concentrations of lead to correct systematic differences in the analysis of low- and high-lead glasses. This may be best achieved by analysing not only reference materials to establish the performance of the spectrometer, but also characterising a subset of the assemblage by an alternate technique. In so doing, a control group is created that allows the identification of elements that are affected by surface conditions or matrix effects, and ultimately provides the means to develop robust empirical calibrations tailored to the assemblage.

In this study, the comparison of pXRF and LA-ICP-MS data for Fe and Sr showed a clear need for the development of different calibration curves for low- and high-lead glasses, in order to lessen some of the effect that high lead concentrations have on pXRF analyses and to make the results internally consistent. In most archaeological scenarios, it will be uncommon to have some 300 samples characterised by LA-ICP-MS to compare the pXRF data with, as in the present study. We expect that in most studies a much smaller number of samples will form the control

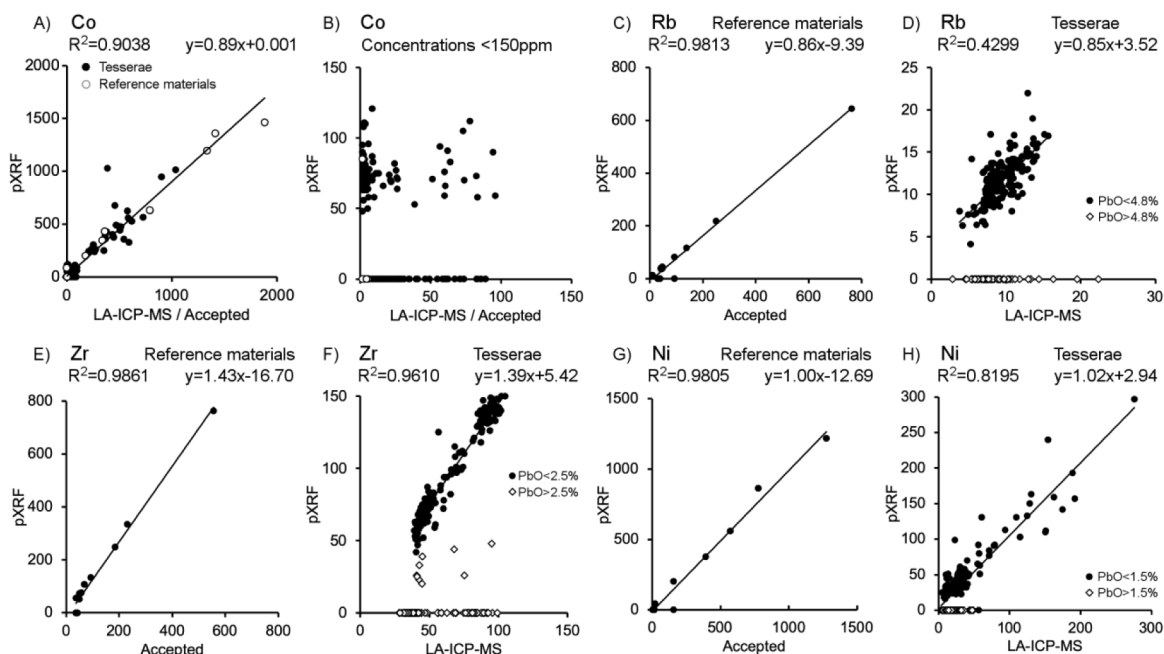


Fig. 6. Comparison of pXRF data with accepted values of reference glasses and with LA-ICP-MS data of archaeological tesserae for elements that were poorly measured or below detection in high lead glasses. The problem is less apparent in the reference materials, which tend to cover a wider range of concentrations and include few high lead glasses. Fig. 6B, D and H also demonstrate the poor precision in the analyses of Co, Rb and Ni when present in low concentrations even in the low-lead tesserae. Concentrations are all in element ppm for this figure.

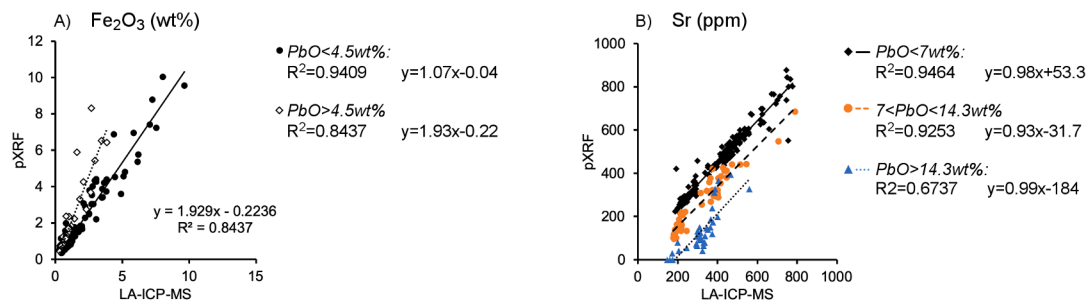


Fig. 7. Tesserae with different concentrations of lead showed different correlations between the pXRF and LA-ICP-MS data, suggesting that different calibrations for low- and high-lead glasses would be beneficial. In the measurement of iron (A), regression analysis of the tesserae with more than 4.5 wt% PbO had a much higher slope. The measurement of Sr (B) shows at least three different groups based on lead content, each with a different linear relationship to the LA-ICP-MS data.

group, in which case the need for separate calibrations based on lead content may not be as evident. Therefore the best and most straightforward approach is to create multiple calibrations for all the elements reported.

As a demonstration of this approach, a subset of 58 samples from the Khirbat al-Minya tesserae were chosen to form a control group for developing empirical calibrations. These samples were preselected and were mounted in resin blocks in an initial phase of the research. Three groups were formed based on the lead content measured by pXRF, with the thresholds determined by breaks observed in the data: glass containing <7 wt% PbO (uncalibrated pXRF data); glass containing between 7 wt% and 18 wt% PbO; and glass containing more than 18 wt% PbO¹. Calibration curves were based upon linear regression analysis using the LA-ICP-MS data as the “true” compositions of the tesserae (designated as the independent variable on the x-axis) to correct the pXRF data (y-axis). A separate calibration curve was generated for each element in each of the three lead groups (e.g., Fig. 8A). The calibrations improved not only the accuracy but the precision of the pXRF analyses, even for elements with acceptable precision pre-calibration. For Sr, the improvement is pronounced. When the calibrations for Sr based on the control group (Fig. 8A) were applied to data for the entire assemblage, the undermeasured Sr contents of the higher lead glass groups were corrected and the accuracy and precision were brought into an acceptable range (compare Fig. 8B and C).

4.2. Applications and usefulness

The usefulness of pXRF for analysing an assemblage containing high lead glasses will depend on the assemblage itself and the research questions of the study, however some comments may be made based on the Khirbat al-Minya tesserae. While identification of different base glass types would be impossible without major elements, compositional groups can be observed in the TiO₂, Sr and Zr concentrations (Fig. 9). A group identified elsewhere as Egypt 1a (Adlington et al., 2020) is compositionally distinct, and while the Levantine and Foy 2.1 groups overlap (in both the pXRF and ICP data), they are mostly separate in their Sr contents in particular. A fourth group referred to as “Low Al₂O₃”, overlaps both the Levantine and Foy 2.1 groups in their TiO₂, Sr and Zr contents, again a problem with both the pXRF and ICP data. Two samples from this group were measured by pXRF as having very high TiO₂ contents, as noted previously (Fig. 2B), which would result in a misidentification during grouping. The single HIMT tessera is clearly

¹ The thresholds between these groups differ from those noted in Fig. 7, as those thresholds were based on the observation of problems in the data for Fe and Sr, and on lead contents measured by LA-ICP-MS. The thresholds in this section are determined solely on lead concentrations (measured by pXRF) of the assemblage, and breaks therein.

distinguished from the rest. While the separation of groups is imperfect, and the information insufficient for pinpointing the specific identity of different primary glass groups, these data could still be useful for guiding sampling decisions for further analysis using more robust techniques.

Aside from compositional grouping, pXRF identifies most of the different colouring and opacifying oxides such as Mn, Fe, Co, Cu, Sn and Pb. Sb, which was well measured in the Noheda samples and reference glasses, was below detection in the Khirbat al-Minya assemblage. Unfortunately, the use of calcium phosphate, used as an opacifier in many of the tesserae, would be very difficult to identify using handheld pXRF. Other technological characteristics could be detected, such as a covariance between lead and tin, evincing the use of lead-tin oxide, and between copper and zinc for the different Egypt 1a colours, indicating the use of a single raw material to create multiple colours.

Handheld pXRF has the potential to be useful in the study of other types of lead glass. Lead was used in this assemblage to aid in the production of specific colours of tesserae, and similarly was used to make strongly coloured beads, glazes and enamels (Beltrán et al., 2020; Brun and Pernot, 1992; Henderson and Warren, 1981; Tite et al., 1998; Tite and Shortland, 2008), although the analysis of glazes and enamels by pXRF may be problematic due to sample thinness. Lead can also be used in glass as a primary fluxing agent, lowering the melting temperature and extending the working time of the molten glass, but also giving the glass a higher refractive index and greater brilliance (Rehren and Freestone, 2015). Lead glass types including lead-barium glass are found in ancient China and in the early Islamic world (Fuxi, 2009; Henderson et al., 2018; Wypyski, 2015). A novel type of Islamic lead glass was recently identified in 8th- to 9th-century al-Andalus (Schibille et al., 2020b) that preceded a specific type of Iberian soda ash lead glass produced locally (de Juan Ares and Schibille, 2017; Duckworth et al., 2015). Lead glasses are also documented in northern Europe during the medieval period (Mecking, 2013), and was used to create lead crystal glass in England in the late seventeenth century (Dungworth, 2019; Dungworth and Brain, 2009).

5. Conclusions

For in situ analysis of ancient and medieval mosaic decorations pXRF presents a viable and as this paper shows, effective method that can identify group affiliations and thus inform sampling and conservation strategies. In view of the varying lead concentrations of glass tesserae, however, the analytical protocol must be optimised, and an empirical calibration is strongly advised. Our study demonstrates how data can be substantially improved by relatively simple adjustments based on linear regression. Best practice for glass studies using pXRF, especially when studying assemblages with variable lead contents, should include not only the analysis of secondary standards, but the analysis of a subset of the assemblage by another, more precise analytical technique. By

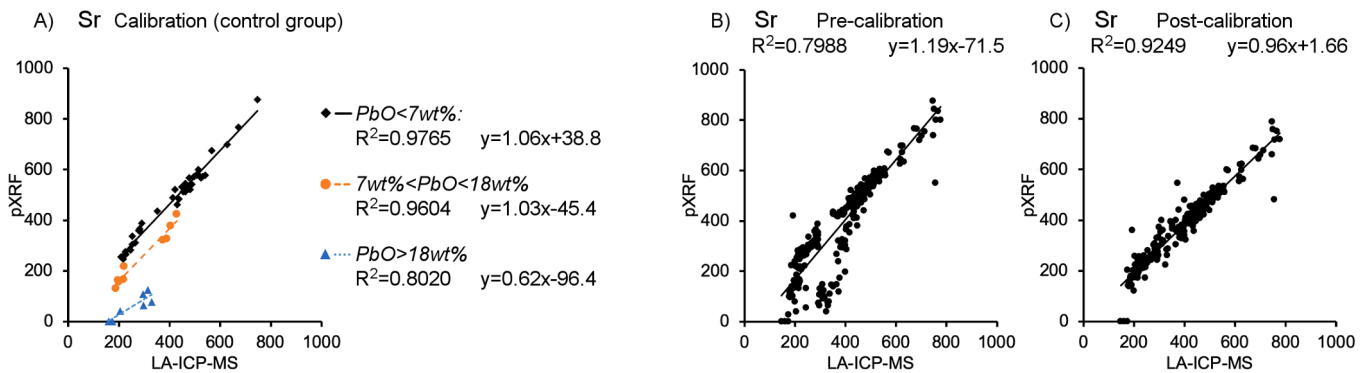


Fig. 8. Graphs showing the application of empirical calibrations to Sr measurements on the Khirbat al-Minya assemblage. (A) Calibration curves were based on linear regression analysis of the low, medium and high lead groups from the control group ($n = 58$). These were applied to the data for the entire assemblage, showing a marked improvement in both the accuracy and precision when compared to the data pre-calibration (B and C). All concentrations are reported in element parts per million.

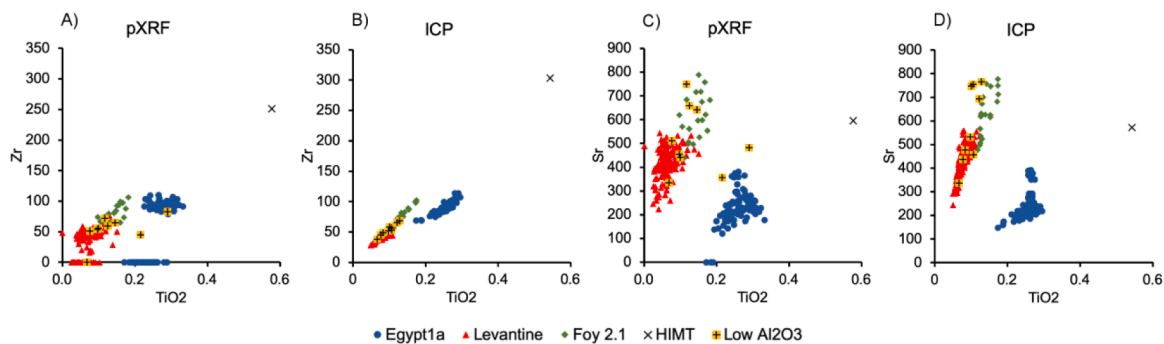


Fig. 9. Graphs comparing pXRF and LA-ICP-MS groupings based on TiO_2 , Sr and Zr, with data coloured based on their primary glass groups as identified based on their major element content. Identification of primary glass groups is currently not feasible using pXRF, but the Egypt 1a and HIMT glass are well distinguished, while the Levantine and Foy 2.1 are mostly separated with some compositional overlap in both the pXRF and the LA-ICP-MS data. The “low Al_2O_3 ” group cannot be distinguished using the limited suite of elements quantifiable by pXRF, and two of this group had outlying TiO_2 contents measured by pXRF that would lead to misidentification of these samples as part of the Egypt 1a group. Therefore four groups are reasonably well distinguished, and the pXRF data could be used to guide sampling decisions for further analysis.

establishing such a control group, it becomes possible to differentiate between surface and matrix effects, and to develop targeted calibrations that should be bracketed based on lead concentrations.

Declaration of Competing Interest

The authors declare that they have no known competing financial interests or personal relationships that could have appeared to influence the work reported in this paper.

Acknowledgements

We are grateful to the Museum of Islamic Art, Berlin, and Professor Markus Ritter for allowing access to the Khirbat al-Minya assemblage and to Miguel Ángel Valero Tévar for access to the Noheda samples. We thank the two anonymous reviewers for their helpful comments on the manuscript. This work was supported by the European Research Council (ERC) under the European Union’s Horizon 2020 research and innovation programme [grant agreement No. 647315 to NS].

Appendix A. Supplementary data

Supplementary data to this article can be found online at <https://doi.org/10.1016/j.jasrep.2020.102603>.

References

- Adlington, L.W., 2019. Making a medieval stained glass window: An archaeometric study of technology and production. Unpublished PhD thesis submitted to UCL Institute of Archaeology.
- Adlington, L.W., 2017. The Corning archaeological reference glasses: New values for “old” compositions. *Pap. Inst. Archaeol.* 27, 1–8. <https://doi.org/10.5334/pia-515>.
- Adlington, L.W., Freestone, I.C., 2017. Using handheld pXRF to study medieval stained glass: A methodology using trace elements. *MRS Adv.* 2, 1785–1800. <https://doi.org/10.1557/adv.2017>.
- Adlington, L.W., Ritter, M., Schibille, N., 2020. Production and provenance of architectural glass from the Umayyad period. *PLoS One* 15 (9), e0239732. <https://doi.org/10.1371/journal.pone.0239732>.
- Arletti, R., Conte, S., Vandini, M., Fiori, C., Bracci, S., Bacci, M., Porcinai, S., 2011. Florence baptistry: Chemical and mineralogical investigation of glass mosaic tesserae. *J. Archaeol. Sci.* 38, 79–88. <https://doi.org/10.1016/j.jas.2010.08.012>.
- Bearden, J.A., 1967. X-ray wavelengths. *Rev. Mod. Phys.* 39, 78–124. <https://doi.org/10.1103/RevModPhys.39.78>.
- Beltrán, M., Schibille, N., Brock, F., Gratuze, B., Vallcorba, O., Pradell, T., 2020. Modernist enamels: Composition, microstructure and stability. *J. Eur. Ceram. Soc.* 40, 1753–1766. <https://doi.org/10.1016/j.jeurceramsoc.2019.11.038>.
- Boschetti, C., Henderson, J., Evans, J., Leonelli, C., 2016. Mosaic tesserae from Italy and the production of Mediterranean coloured glass (4th century BCE–4th century CE). Part I: Chemical composition and technology. *J. Archaeol. Sci. Rep.* 7, 303–311. <https://doi.org/10.1016/j.jasrep.2016.05.006>.
- Brand, N.W., Brand, C.J., 2014. Performance comparison of portable XRF instruments. *Geochem. Explor. Environ. Anal.* 14, 125–138.
- Brill, R.H., 1999. *Chemical Analyses of Early Glasses*. Corning Museum of Glass, Corning, NY.
- Brun, N., Pernot, M., 1992. The opaque red glass of Celtic enamels from Continental Europe. *Archaeometry* 34, 235–252.

- Bugoi, R., Poll, I., Mănuclu-Adameșteanu, G., Calligaro, T., Pichon, L., Pacheco, C., 2016. PIXE-PIGE analyses of Byzantine glass bracelets (10th–13th centuries AD) from Isaccoea, Romania. *J. Radioanal. Nucl. Chem.* 307, 1021–1036. <https://doi.org/10.1007/s10967-015-4240-0>.
- Craig, N., Speakman, R.J., Popelka-Filcoff, R.S., Glascock, M.D., Robertson, J.D., Shackley, M.S., Aldenderfer, M.S., 2007. Comparison of XRF and pXRF for analysis of archaeological obsidian from southern Perú. *J. Archaeol. Sci.* 34, 2012–2024. <https://doi.org/10.1016/j.jas.2007.01.015>.
- de Juan Ares, J., Schibille, N., 2017. Glass import and production in Hispania during the early medieval period: The glass from Ciudad de Vascos (Toledo). *PLoS One* 12, 1–19. <https://doi.org/10.1371/journal.pone.0182129>.
- de Viguier, L., Duran, A., Bouquillon, A., Solé, V.A., Castaing, J., Walter, P., 2009. Quantitative X-ray fluorescence analysis of an Egyptian faience pendant and comparison with PIXE. *Anal. Bioanal. Chem.* 395, 2219–2225. <https://doi.org/10.1007/s00216-009-2974-7>.
- Duckworth, C.N., de la Llave, R.C., Faber, E.W., Edwards, D.J.G., Henderson, J., 2015. Electron microprobe analysis of 9th–12th-century Islamic glass from Córdoba, Spain. *Archaeometry* 57, 27–50. <https://doi.org/10.1111/arc.12079>.
- Dungworth, D., 2019. Glassworking in England from the 14th to the 20th Century. *Historic England, Swindon, UK*.
- Dungworth, D., 2012. Historic windows: Investigation of composition groups with nondestructive pXRF. *Glas. Technol. Eur. J. Glas. Sci. Technol. Part A* 53, 192–197.
- Dungworth, D., Brain, C., 2009. Late 17th-century crystal glass: An analytical investigation. *J. Glass Stud.* 51, 111–137.
- Dussubieux, L., 2016. A proficiency test for LA-ICP-MS laboratories analyzing ancient glass. In: Dussubieux, L., Golitko, M., Gratuze, B. (Eds.), *Recent Advances in Laser Ablation ICP-MS for Archaeology*. Springer, Berlin, pp. 197–212.
- Frahm, E., 2013. Validity of “off-the-shelf” handheld portable XRF for sourcing Near Eastern obsidian chip debris. *J. Archaeol. Sci.* 40, 1080–1092. <https://doi.org/10.1016/j.jas.2012.06.038>.
- Fuxi, G., 2009. Origin and evolution of ancient Chinese glass. In: Fuxi, G., Brill, R.H., Shouyun, T. (Eds.), *Ancient Glass Research along the Silk Road*. World Scientific Publishing, Singapore.
- Gabler, C. V., 2017. Craft Production and Exchange in the Pre-Hispanic Andes: LA-ICP-MS and pXRF Analyses of Tiwanaku Ceramics. Georgia State University.
- Goodale, N., Bailey, D.G., Jones, G.T., Prescott, C., Scholz, E., Stagliano, N., Lewis, C., 2012. pXRF: A study of inter-instrument performance. *J. Archaeol. Sci.* 39, 875–883. <https://doi.org/10.1016/j.jas.2011.10.014>.
- Gratuze, B., 1999. Obsidian characterization by laser ablation ICP-MS and its application to prehistoric trade in the Mediterranean and the Near East: Sources and distribution of obsidian within the Aegean and Anatolia. *J. Archaeol. Sci.* 26, 869–881. <https://doi.org/10.1006/jasc.1999.0459>.
- Grave, P., Attenbrow, V., Sutherland, L., Pogson, R., Forster, N., 2012. Non-destructive pXRF of mafic stone tools. *J. Archaeol. Sci.* 39, 1674–1686. <https://doi.org/10.1016/j.jas.2011.11.011>.
- Heginbotham, A., Bourgarit, D., Day, J., Dorscheid, J., Godla, J., Lee, L., Pappot, A., Robcis, D., 2019. Charmed PyMCA, Part II: An evaluation of interlaboratory reproducibility for ED-XRF analysis of copper alloys. *Archaeometry*. <https://doi.org/10.1111/arc.12488>.
- Heginbotham, A., Solé, V.A., 2017. CHARMed PyMca Part I: A protocol for improved inter-laboratory reproducibility in the quantitative ED-XRF analysis of copper alloys. *Archaeometry*. <https://doi.org/10.1111/arc.12282>.
- Henderson, J., An, J., Ma, H., 2018. The archaeometry and archaeology of ancient Chinese glass: A review. *Archaeometry* 60, 88–104. <https://doi.org/10.1111/arc.12368>.
- Henderson, J., Warren, S.E., 1981. X-ray fluorescence analyses of Iron Age glass: Beads from Meare and Glastonbury Lake villages. *Archaeometry* 23, 83–94.
- Janssens, K., Van der Snickt, G., Vanmeert, F., Legrand, S., Nuyts, G., Alfeld, M., Monico, L., Anaf, W., De Nolf, W., Vermeulen, M., Verbeeck, J., De Wael, K., 2016. Non-invasive and non-destructive examination of artistic pigments, paints, and paintings by means of X-ray methods. *Top. Curr. Chem.* 374, 1–52. <https://doi.org/10.1007/978-3-319-52804-5>.
- Jochum, K.P., Weis, U., Stoll, B., Kuzmin, D., Yang, Q., Raczek, I., Jacob, D.E., Stracke, A., Birbaum, K., Frick, D.A., Günther, D., Enzweiler, J., 2011. Determination of reference values for NIST SRM 610–617 glasses following ISO guidelines. *Geostand. Geoanalytical Res.* 35, 397–429. <https://doi.org/10.1111/j.1751-908X.2011.00120.x>.
- Kaiser, B., Shugar, A.N., 2012. Glass analysis utilizing handheld X-ray fluorescence. In: Shugar, A.N., Mass, J.L. (Eds.), *Handheld XRF for Art and Archaeology, Studies in Archaeological Sciences*. Leuven University Press, Leuven, Belgium, pp. 449–470.
- Koleini, F., Colomban, P., Antonites, A., Pikirayi, I., 2017. Raman and XRF classification of Asian and European glass beads recovered at Mutamba, a southern African Middle Iron Age site. *J. Archaeol. Sci. Rep.* 13, 333–340. <https://doi.org/10.1016/j.jasrep.2017.04.004>.
- Koleini, F., Colomban, P., Pikirayi, I., 2020. Post-15th century European glass beads in southern Africa: Composition and classification using pXRF and Raman spectroscopy. *J. Archaeol. Sci. Rep.* 29, 102183. <https://doi.org/10.1016/j.jasrep.2019.102183>.
- Lahlil, S., Biron, I., Galois, L., Morin, G., 2008. Rediscovering ancient glass technologies through the examination of opacifier crystals. *Appl. Phys. A Mater. Sci. Process.* 92, 109–116. <https://doi.org/10.1007/s00339-008-4456-8>.
- Lahlil, S., Cotte, M., Biron, I., Szlachetko, J., Menguy, N., Susini, J., 2011. Synthesizing lead antimonate in ancient and modern opaque glass. *J. Anal. At. Spectrom.* 2011 (26), 1040–1050. <https://doi.org/10.1039/c0ja00251h>.
- Liritzis, I., Zacharias, N., 2011. Portable XRF of archaeological artifacts: Current research, potentials and limitations, in: Shackley, M.S. (Ed.), *X-Ray Fluorescence Spectrometry (XRF) in Geoarchaeology*. Springer, New York, pp. 109–142. <https://doi.org/10.1017/CBO9781107415324.004>.
- Licenziati, F., Calligaro, T., 2016. Study of mosaic glass tesserae from Delos, Greece using a combination of portable μ -Raman and X-ray fluorescence spectrometry. *J. Archaeol. Sci. Rep.* 7, 640–648. <https://doi.org/10.1016/j.jasrep.2015.10.017>.
- Mao, Y., 2000. Lead-alkaline glazed Egyptian faience: Preliminary technical investigation of Ptolemaic period faience vessels in the collection of the Walters Art Gallery. *J. Am. Inst. Conserv.* 39, 185–204. <https://doi.org/10.1179/019713600806082739>.
- Martín-Torres, M., Li, X.J., Bevan, A., Xia, Y., Zhao, K., Rehren, T., 2012. Forty thousand arms for a single emperor: From chemical data to the labor organization behind the bronze arrows of the terracotta army. *J. Archaeol. Method Theory* 21, 534–562. <https://doi.org/10.1007/s10816-012-9158-z>.
- Matin, M., Tite, M.S., Watson, O., 2018. On the origins of tin-opacified ceramic glazes: New evidence from early Islamic Egypt, the Levant, Mesopotamia, Iran, and Central Asia. *J. Archaeol. Sci.* 97, 42–66. <https://doi.org/10.1016/j.jas.2018.06.011>.
- Mecking, O., 2013. Medieval lead glass in central Europe. *Archaeometry* 55, 640–662. <https://doi.org/10.1111/j.1475-4754.2012.00697.x>.
- Meek, A., 2016. Ion beam analysis of glass inlays from the Staffordshire Anglo-Saxon Hoard. *J. Archaeol. Sci. Rep.* 7, 324–329. <https://doi.org/10.1016/j.jasrep.2016.05.014>.
- Neri, E., Biron, I., Verità, M., 2018. New insights into Byzantine glass technology from loose mosaic tesserae from Hierapolis (Turkey): PIXE/PIGE and EPMA analyses. *Archaeol. Anthropol. Sci.* 10, 1751–1768. <https://doi.org/10.1007/s12520-017-0492-7>.
- O’Grady, C., Hurst, H., 2011. Lost walls/murals rebuilt: Interdisciplinary approaches to the conservation of preclassical Maya Wall Paintings from San Bartolo, Guatemala. In: Bridgland, J. (Ed.), *ICOM-CC 16th Triennial Preprints - Lisbon*. ICOM, Portugal, pp. 1–10.
- Potts, P.J., Webb, P.C., Williams-Thorpe, O., 1997. Investigation of a correction procedure for surface irregularity effects based on scatter peak intensities in the field analysis of geological and archaeological rock samples by portable X-ray fluorescence spectrometry. *J. Anal. At. Spectrom.* 12, 769–776.
- Rehren, Th., Freestone, I.C., 2015. Ancient glass: from kaleidoscope to crystal ball. *J. Archaeol. Sci.* 56, 233–241. <https://doi.org/10.1016/j.jas.2015.02.021>.
- Ritter, M., 2017. Der umayyadische Palast des 8. Jahrhunderts in Hīrbat al-Minya am See von Tiberias: Bau und Baudekor. Reichert Verlag, Wiesbaden.
- Robinet, L., Bouguillon, A., Hartwig, J., 2008. Correlations between Raman parameters and elemental composition in lead and lead alkali silicate glasses. *J. Raman Spectrosc.* 39, 618–626. <https://doi.org/10.1002/jrs>.
- Roxburgh, M.A., Heeren, S., Huisman, D.J., Van Os, B.J.H., 2018. Non-destructive survey of early Roman copper-alloy brooches using portable X-ray fluorescence spectrometry. *Archaeometry*. <https://doi.org/10.1111/arc.12414>.
- Schibille, N., Boschetti, C., Valero Tévar, M.A., Veron, E., de Juan Ares, J., 2020a. The color palette of the mosaics in the Roman Villa of Noheda (Spain). *Minerals* 10, 272. <https://doi.org/10.3390/min10030272>.
- Schibille, N., de Juan Ares, J., Casal García, M.T., Guerot, C., 2020b. Ex novo development of lead glassmaking in early Umayyad Spain. *Proc. Natl. Acad. Sci.* 117. <https://doi.org/10.1073/pnas.2003440117>.
- Schibille, N., Neri, E., Ebanista, C., Ramzi, M., Bisconti, F., 2018. Something old, something new: The late antique mosaics from the catacomb of San Gennaro (Naples). *J. Archaeol. Sci. Rep.* 20, 411–422. <https://doi.org/10.1016/j.jasrep.2018.05.024>.
- Scott, R.B., Braekmans, D., Brems, D., Degryse, P., 2012. Danger! High voltage! The application of handheld X-ray fluorescence (HH-XRF) to experimental glass: Pitfalls and potentials. *Proc. 39th Int. Symp. Archaeom. Leuven* 268–273.
- Shackley, M.S., 2010. Is there reliability and validity in portable X-ray fluorescence spectrometry (pXRF)? *SAA Archaeol. Rec.* 10, 17–20.
- Sheppard, P.J., Irwin, G.J., Lin, S.C., McCaffrey, C.P., 2011. Characterization of New Zealand obsidian using pXRF. *J. Archaeol. Sci.* 38, 45–56. <https://doi.org/10.1016/j.jas.2010.08.007>.
- Shortland, A.J., 2002. The use and origin of antimonate colorants in early Egyptian glass. *Archaeometry* 44, 517–530. <https://doi.org/10.1111/1475-4754.t01-1-00083>.
- Silvestri, A., Tonietto, S., Molin, G., Guerriero, P., 2014. The palaeo-Christian glass mosaic of St. Prodocimus (Padova, Italy): archaeometric characterisation of tesserae with copper- or tin-based opacifiers. *J. Archaeol. Sci.* 42, 51–67. <https://doi.org/10.1016/j.jas.2013.10.018>.
- Speakman, R.J., Shackley, M.S., 2013. Silo science and portable XRF in archaeology: A response to Frahm. *J. Archaeol. Sci.* 40, 1435–1443. <https://doi.org/10.1016/j.jas.2012.09.033>.
- Stroth, L., Otto, R., Daniels, J.T., Braswell, E., 2019. Statistical artifacts: Critical approaches to the analysis of obsidian artifacts by portable X-ray fluorescence. *J. Archaeol. Sci. Rep.* 24, 738–747. <https://doi.org/10.1016/j.jasrep.2019.02.023>.
- Tesser, E., Verità, M., Lazzarini, L., Falcone, R., Sagul, L., Antonelli, F., 2020. Glass in imitation of exotic marbles: An analytical investigation of 2nd century AD Roman sectilia from the Gorga collection. *J. Cult. Herit.* 42, 202–212. <https://doi.org/10.1016/j.culher.2019.07.009>.
- Tite, M.S., Freestone, I.C., Mason, R., Molera, J., Vendrell-Saz, M., Wood, N., 1998. Lead glazes in antiquity - Methods of production and reasons for use. *Archaeometry* 40, 241–260.
- Tite, M.S., Shortland, A., 2008. Discovery, production and use of tin-based opacifiers in glasses, enamels and glazes from the Late Iron Age onwards: A reassessment. *Archaeometry* 50, 67–84. <https://doi.org/10.1111/j.1475-4754.2007.00339.x>.
- Tykot, R.H., 2016. Using nondestructive portable X-ray fluorescence spectrometers on stone, ceramics, metals, and other materials in Museums: Advantages and

- limitations. *Appl. Spectrosc.* 70, 42–56. <https://doi.org/10.1177/0003702815616745>.
- Verità, M., Biron, I., Cagnini, A., Porcinai, S., Barbe, F., 2018. The so-called Venetian enamelled copper artworks of the Italian Renaissance: The technology and provenance of the enamels—An analytical approach. *Archaeometry* 60, 233–254. <https://doi.org/10.1111/arcn.12312>.
- Wagner, B., Nowak, A., Bulska, E., Hametner, K., Günther, D., 2012. Critical assessment of the elemental composition of Corning archeological reference glasses by LA-ICP-MS. *Anal. Bioanal. Chem.* 402, 1667–1677. <https://doi.org/10.1007/s00216-011-5597-8>.
- Wilke, D., Rauch, D., Rauch, P., 2016. Is non-destructive provenancing of pottery possible with just a few discriminative trace elements? *STAR Sci. Technol. Archaeol. Res.* 1–18. <https://doi.org/10.1080/20548923.2016.1209030>.
- Williams-Thorpe, O., Potts, P.J., Webb, P.C., 1999. Field-portable non-destructive analysis of lithic archaeological samples by X-Ray fluorescence instrumentation using a mercury iodide detector: Comparison with wavelength-dispersive XRF and a case study in British Stone Axe Provenancing. *J. Archaeol. Sci.* 26, 215–237. <https://doi.org/10.1006/jasc.1998.0323>.
- Wypyski, M.T., 2015. Chemical analysis of early Islamic glass from Nishapur. *J. Glass Stud.* 57, 121–136.
- Wypyski, M.T., 2005. Technical analysis of glass mosaic tesserae from Amorium. *Dumbart. Oaks Pap.* 59, 183–192.
- Živković, J., Power, T., Georgakopoulou, M., López, J.C.C., 2019. Defining new technological traditions of Late Islamic Arabia: A view on Bahlā Ware from al-Ain (UAE) and the lead-barium glaze production. *Archaeol. Anthropol. Sci.* 11, 4697–4709. <https://doi.org/10.1007/s12520-019-00807-6>.
- Zucchiatti, A., Bouquillon, A., Lanterna, G., Lucarelli, F., Andrea Mandò, P., Prati, P., Salomon, J., Grazia Vaccari, M., 2002. PIXE and μ -PIXE analysis of glazes from terracotta sculptures of the della Robbia workshop. *Nucl. Inst. Methods Phys. Res. SectB Beam Interact. Mater. Atoms* 189, 358–363. [https://doi.org/10.1016/S0168-583X\(01\)01087-4](https://doi.org/10.1016/S0168-583X(01)01087-4).